frontiers in Built Environment

ORIGINAL RESEARCH
published: 26 May 2017
doi: 10.3389/fbuil.2017.00031

Robustness Evaluation of Elastoplastic Base-Isolated High-Rise Buildings Subjected to Critical Double Impulse

*Kohei Fujita[1], Keisuke Yasuda[1], Yoshihiro Kanno[2] and Izuru Takewaki[1]**

[1] Department of Architecture and Architectural Engineering, Graduate School of Engineering, Kyoto University, Kyoto, Japan, [2] Laboratory for Future Interdisciplinary Research of Science and Technology, Institute of Innovative Research, Tokyo Institute of Technology, Yokohama, Japan

A new method of robustness evaluation is proposed for an elastoplastic base-isolated high-rise building considering simultaneous uncertainties of structural parameters. Since it is difficult to evaluate the robustness of elastoplastic structures due to heavy computational load on the time-history response analysis including elastoplastic response, a double impulse input is used to provide a closed-form solution of the critical response of a single-degree-of-freedom (SDOF) elastic–perfectly plastic structure under a near-field ground motion. Introducing an equivalent elastoplastic SDOF model of a base-isolated high-rise building, the worst combination of uncertain structural parameters, i.e., the stiffness and yield deformation at the base-isolation story and the stiffness of the superstructure, can be derived which leads to the upper bound of the critical elastoplastic response. It is shown that, by using the derived upper bound of the critical response, the robustness function, a measure of the robustness, of elastoplastic structures can be evaluated efficiently. In numerical examples, the robustness of a 30-story base-isolated high-rise building is compared with those of other models with different yield deformations at the base-isolation story to find a preferable design with larger robustness.

Keywords: robustness evaluation, critical response, double impulse, base-isolated building, elastoplastic response, robust design

OPEN ACCESS

Edited by:
Fabio Mazza, University of Calabria, Italy

Reviewed by:
Tao Wang, China Earthquake Administration, China
Naohiro Nakamura, Hiroshima University, Japan
Iolanda-Gabriela Craifaleanu, Technical University of Civil Engineering of Bucharest, Romania

****Correspondence:***
Izuru Takewaki
takewaki@archi.kyoto-u.ac.jp

Specialty section:
This article was submitted to Earthquake Engineering, a section of the journal Frontiers in Built Environment

Received: *23 March 2017*
Accepted: *05 May 2017*
Published: *26 May 2017*

Citation:
Fujita K, Yasuda K, Kanno Y and Takewaki I (2017) Robustness Evaluation of Elastoplastic Base-Isolated High-Rise Buildings Subjected to Critical Double Impulse. Front. Built Environ. 3:31. doi: 10.3389/fbuil.2017.00031

INTRODUCTION

To enhance the structural safety of buildings, the variation of their structural performances with respect to various uncertainties should be evaluated from the view point of robustness. Uncertainties of design ground motions and structural parameters resulting from various sources, e.g., unpredictability of natural phenomena, material-property variability, initial manufacturing error, aging deterioration of performance, are of great concern in assessing the structural performances. In particular, the isolators, e.g., natural rubber bearing (NRB), used for base-isolated buildings have large variations of structural properties and should be used with careful attention. It is therefore desired to evaluate these variations of structural performances efficiently.

The interval evaluation methods of structural performances based on a probabilistic or non-probabilistic approach have been studied extensively (Ben-Haim and Elishakoff, 1990; Ben-Haim et al., 1996; Qiu and Wang, 2003; Elishakoff and Ohsaki, 2010; Fujita and Takewaki, 2011; Roy et al., 2012; Guo and Li, 2013; Han et al., 2014; Yang et al., 2015, 2017). Furthermore, the robustness

evaluation methods have been proposed as advanced methods for evaluating the toughness of structures under various uncertain circumstances. A number of studies on the robustness evaluation methods and its application to the robust design have been discussed for various building models (Kanno and Takewaki, 2006; Matsuda and Kanno, 2008; Takewaki, 2008; Tsompanakis et al., 2008; Fujita and Takewaki, 2012).

A non-probabilistic robustness index, called the robustness function, was introduced by Ben-Haim (2006) based on the so-called info-gap model to evaluate the structural robustness as a quantitative index. The robustness function can be defined as the maximum allowable uncertainty level in parameters to satisfy the specified structural performance demand. In this formulation, the interval parameter is one of the non-probabilistic uncertain-but-bounded parameters based on the info-gap model. By using the abovementioned structural uncertainties and the robustness function, the robustness with respect to various structural performances in various structural models has been investigated so far (Takewaki and Ben-Haim, 2005; Kanno and Takewaki, 2006; Matsuda and Kanno, 2008; Fujita and Takewaki, 2011). Although the robustness using the robustness function has been studied extensively, most object structures were modeled as elastic structures. Since the evaluation of the maximum elastoplastic deformation of structures using time-history response analysis is too time-consuming, a few references can be found in this field.

To take into account the uncertainty of earthquake ground motions in a reliable manner, it may be important to find the critical excitation which maximizes the structural responses. As a simplified pulse-type model of near-fault ground motions, Kojima and Takewaki (2015) introduced the double impulse input and derived the critical input interval, which maximizes the peak elastoplastic response. In the theory of critical double impulse input, a closed-form solution of the critical response, i.e., the maximum elastoplastic displacement, to this critical double impulse input has been formulated for an undamped elastoplastic single-degree-of-freedom (SDOF) model. By using this closed-form solution of the critical elastoplastic response, Kanno and Takewaki (2016) and Kanno et al. (2017) investigated the robustness evaluation method for elastoplastic structures under the simultaneous structural uncertainties. However, since the closed-form solution of the elastoplastic displacement proposed by Kojima and Takewaki (2015) is applicable only to SDOF models, the structural uncertainties are limited to two parameters, i.e., only the fundamental natural frequency and yield deformation.

In this paper, the robustness evaluation method for base-isolated high-rise buildings is presented where simultaneous uncertainties are considered for both the elastoplastic property, i.e., stiffness and yield deformation, of the base-isolation story and the stiffness of the superstructure. The base-isolated high-rise building is treated first as a two DOF model. To apply the closed-form solution of the elastoplastic displacement of an SDOF model, the two DOF model is transformed first into an equivalent elastoplastic SDOF model. The upper bounds of the critical elastoplastic response of the base-isolation story and the elastic response of the superstructure are derived where the worst case scenario of the uncertain structural parameters are investigated in detail. Finally, by applying the derived supremum value of the upper bound of the critical elastoplastic responses to the objective function of the robustness function, the robustness of the base-isolated building is evaluated for several yield deformations at the base-isolation story. It is shown through numerical examples that a preferable design of the nominal yield deformation at the base-isolation story exists in base-isolated high-rise buildings to make the robustness in terms of elastoplastic structural responses larger.

MAXIMUM ELASTOPLASTIC RESPONSE UNDER CRITICAL DOUBLE IMPULSE INPUT

In this section, a simplified response evaluation method used for the robustness evaluation is briefly explained where the maximum elastoplastic response of an SDOF elastic–perfectly plastic structure under the critical double impulse is expressed in closed form.

Kojima and Takewaki (2015) introduced the double impulse to represent the principal part of a pulse-type near-fault ground motion and derived the closed-form maximum elastoplastic response of an SDOF structure by considering the energy balance and the critical timing of the double impulse. **Figure 1** shows an example of the double impulse compared with one-cycle sine wave. Let us consider an undamped elastic–perfectly plastic SDOF system with ω and d_y as the undamped natural circular frequency and the yield deformation, respectively. The double impulse can be described by the following equation:

$$\ddot{u}_g(t) = V\delta(t) - V\delta(t - t_0) \tag{1}$$

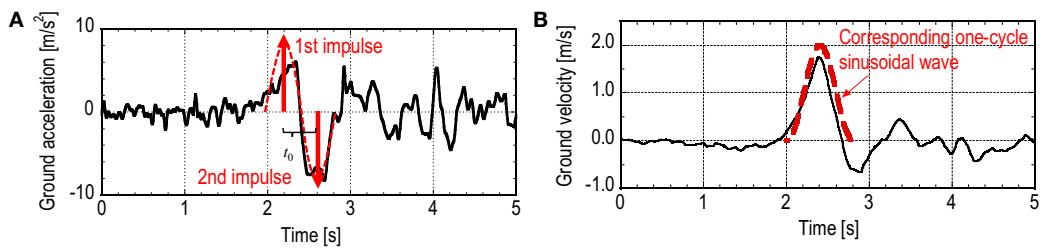

FIGURE 1 | One-cycle sine wave as representative of principal part of near-fault ground motion and double impulse (Rinaldi station fault-normal component, Northridge 1994) (A) acceleration, (B) velocity.

where V, t_0, and $\delta(t)$ denote the amplitude (velocity level) of impulse, the time interval between the first and second impulses, and the Dirac delta function, respectively. It has been shown that there exists the critical time interval t_0^c for a given input level V, which maximizes the elastoplastic deformation of the SDOF system. In the past study, it was made clear that t_0^c is the time when the restoring force of the SDOF system after the first impulse becomes 0. Let $w^{(1)}$ and $w^{(2)}$ denote the absolute value of the maximum deformation after the first and second impulses, respectively. Then, the maximum elastoplastic deformation of the SDOF system can be obtained as max $\{w^{(1)}, w^{(2)}\}$. This maximum deformation is defined as the critical response w^c. By specifying t_0^c and V, u^c can be derived from the energy balance as follows:

$$w^c(\omega; d_y; V) = \begin{cases} (2/\omega)V & (0 < V \le V_y/2) \\ \left\{2/(\omega^2 d_y)\right\} V^2 + (1/2)d_y & (V_y/2 < V \le V_y) \\ (1/\omega)V + (3/2)d_y & (V_y < V \le (\sqrt{3}+1)V_y) \\ \left\{1/(2\omega^2 d_y)\right\} V^2 + (1/2)d_y & ((\sqrt{3}+1)V_y < V) \end{cases} \quad (2)$$

where V_y is defined as the velocity at which the structure just yields after the first impulse and ω denotes the natural circular frequency of the SDOF system using initial elastic stiffness. Therefore, V_y represents the strength of the SDOF system given by $V_y = \omega d_y$ with d_y being the yield deformation. In Eq. 2, w^c is categorized by the input level V. This is because the energy balance equation of the elastoplastic deformation exhibits different situations according to the amplitude of V. By substituting $V_y = \omega d_y$ in Eq. 2, the inequality equations can be described in terms of either ω or d_y. From the observation of the variation of w^c, Kanno et al. (2017) showed the monotonicity of w^c with respect to ω and the non-monotonicity of w^c with respect to d_y. **Figure 2** shows the variation of w^c with respect to d_y for a fixed ω. It has been shown that w^c can be minimized at $w^{(1)} = w^{(2)}$.

UPPER BOUND OF DISPLACEMENT OF ELASTOPLASTIC BASE-ISOLATED HIGH-RISE BUILDING UNDER SIMULTANEOUS UNCERTAINTIES IN STRUCTURAL PARAMETERS

To evaluate the robustness of elastoplastic base-isolated high-rise buildings for various uncertainties, it is desired to obtain the maximum structural response without large computational load. Kanno et al. (2017) presented the robustness evaluation method using an SDOF model subjected to the critical double impulse. It was shown that, by using the closed-form solution of the maximum elastoplastic displacement derived by Kojima and Takewaki (2015), the robustness of the SDOF model exhibiting elastoplastic responses can be derived efficiently. However, in the previous study, only two parameters, i.e., the yield deformation and the natural frequency of the SDOF model, were treated as uncertain parameters. To apply the robustness evaluation method using the critical double impulse to a practical building model, a base-isolated high-rise building is considered in this paper.

Relationship between Equivalent SDOF Model and 2DOF Base-Isolated Building Model

As a simplified structural model of a base-isolated building, a 2DOF model is often used in the seismic analysis where the masses of the superstructure are reduced to a single mass (Naeim and Kelly, 1999). Furthermore, to apply the closed-form solution of the critical elastoplastic displacement as shown in Eq. 2, it is necessary that a 2DOF model is further reduced to an equivalent SDOF model (**Figure 3**).

Let m_1, k_1, and d_{y1} denote the mass, elastic stiffness, and yield deformation of the base-isolation story, respectively. In addition, let m_2 and k_2 denote the mass and stiffness of the superstructure, respectively. The restoring-force characteristic of the base-isolation story is assumed to be elastic–perfectly plastic. This is

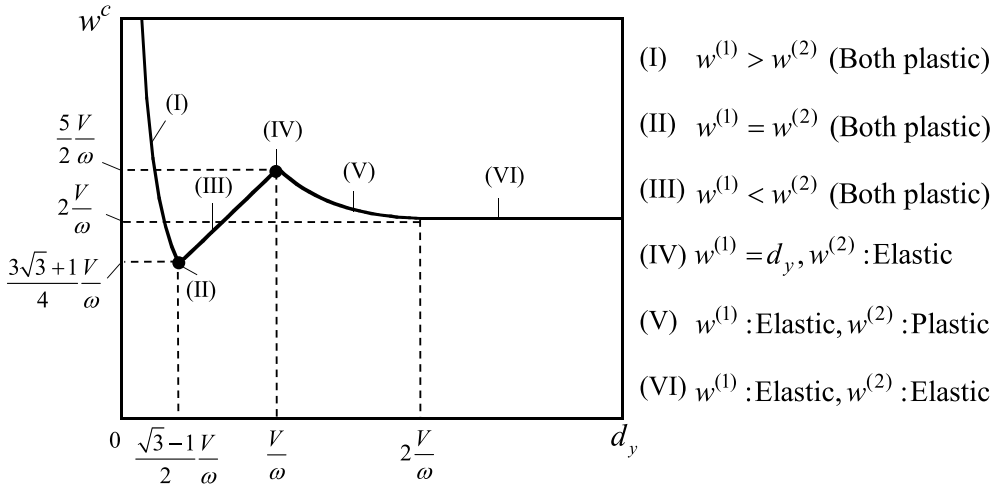

FIGURE 2 | Non-monotonicity property of critical elastoplastic response with respect to yield deformation.

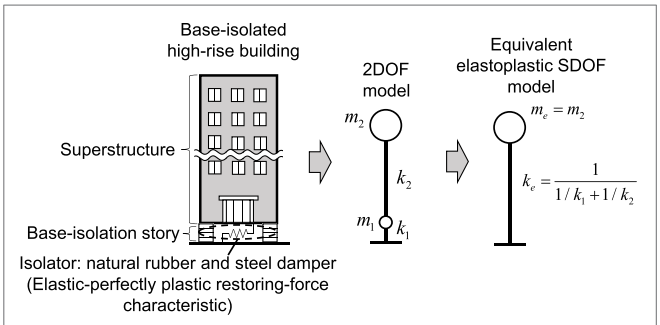

FIGURE 3 | Simplified model of base-isolated high-rise building.

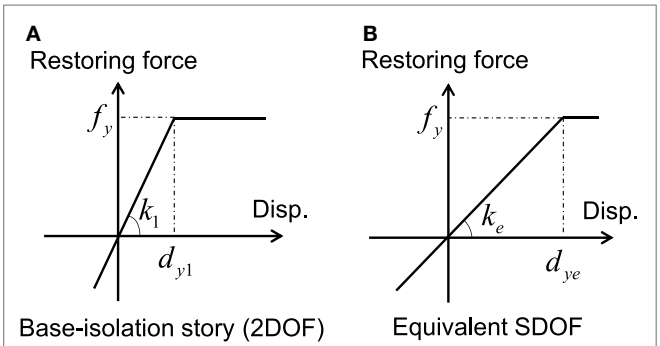

FIGURE 4 | Restoring force–displacement relations of simplified structural models: (A) 2DOF model, (B) single-degree-of-freedom (SDOF) model.

a simple model of the combination of natural rubbers and steel dampers. The elastic–perfectly plastic structure model can be regarded as a simplified model with safer margin. This is because the seismic response of the elastic–perfectly plastic model may often be larger than that of the bilinear model considering secondary stiffness. On the other hand, the superstructure is regarded to be elastic due to the seismic response reduction by base-isolation. Since the mass of the base-isolation story is relatively small compared with that of the high-rise superstructure, the mass m_e of the equivalent SDOF model can be given by m_2, i.e., m_1 is neglected. The equivalent stiffness k_e of the SDOF model can be given as the series model of k_1 and k_2 by the following equation:

$$k_e = \frac{k_1 k_2}{k_1 + k_2} \tag{3}$$

Then, the equivalent natural circular frequency ω_e can be obtained as $\omega_e = \sqrt{k_e/m_e}$. Therefore, ω_e is a function of k_1 and k_2. A closed-form solution, Eq. 2, for the SDOF model was derived by ignoring the inherent damping. It seems that this approximation provides a larger response than that of the model with the inherent damping. Therefore, the inherent damping is neglected here.

Figure 4 shows the restoring-force relation of the 2DOF model and the equivalent SDOF model. Since the yield forces of those models are the same due to the simplification using a series model, the equivalent yield deformation d_{ye} can be derived by the following equation:

$$d_{ye} = d_{y1}\left(1 + \frac{k_1}{k_2}\right) \tag{4}$$

Finally, by substituting ω_e and d_{ye} of the equivalent SDOF model into Eq. 2, the maximum elastoplastic displacement of the base-isolated high-rise building model subjected to the critical double impulse can be obtained in the closed-form.

In base-isolated high-rise buildings, the investigation on higher-mode effects and overturning effects may be necessary. It should be noted that, while the story shear forces are highly influenced by higher-modes, their effects on the building top displacement and the isolation-story displacement are rather limited. These will be discussed in the future. Because the principal purpose of the present paper is to focus on the robustness analysis of base-isolated high-rise buildings with plastic deformation, a rather simplified model enabling the derivation of closed-form expression of the maximum response is used. The relationship between the 2DOF model and the SDOF model is discussed in Appendix (Taniguchi et al., 2016a,b).

Closed-Form Expression of Upper Bound of Maximum Critical Elastoplastic Response

In this section, the upper bound of the maximum critical elastoplastic displacement $w^c(\omega_e; d_{ye}; V)$ of the equivalent SDOF model is investigated with respect to simultaneous uncertainties of k_1, k_2, and d_{y1}. In the following formulations, the maximum critical elastoplastic displacement for a fixed input level V is treated as a function of k_1, k_2, and d_{y1}. Therefore, we redefine it as $u^c(k_1; k_2; d_{y1})$ instead of $w^c(\omega_e; d_{ye}; V)$ in Eq. 2. While the maximum displacement u^c means the maximum value with respect to time, the upper bound of u^c represents the maximum value of u^c in the structural uncertainties.

The uncertain parameters k_1, k_2, and d_{y1} are given by the interval parameters based on the info-gap model (Ben-Haim, 2006). The interval parameters k_1, k_2, and d_{y1} are bounded in terms of the upper and lower bounds of each parameter as follows:

$$\begin{aligned} 0 < \underline{k}_1 \le k_1 \le \bar{k}_1 \\ 0 < \underline{k}_2 \le k_2 \le \bar{k}_2 \\ 0 < \underline{d}_{y1} \le d_{y1} \le \bar{d}_{y1} \end{aligned} \tag{5a,b,c}$$

where the upper and lower bar symbols denote the upper and lower limits, respectively, of the interval parameters.

To derive the upper bound of u^c with respect to simultaneous uncertainties of k_1, k_2, and d_{y1}, it is important to understand first the property of u^c with respect to the variation of k_1 and k_2. In Eq. 2, w^c (u^c in this section) can be regarded as an increasing function of $1/\omega$ in all categories. Therefore, if d_{ye} is fixed as a constant value during the variation of k_1 and k_2 in Eq. 2, it is evident that u^c decreases with respect to the increase of ω. Furthermore, since $\partial k_e/\partial k_1 = (k_2/k_1 + k_2)^2 > 0$, $\partial k_e/\partial k_2 = (k_1/k_1 + k_2)^2 > 0$ are derived from Eq. 3, the monotonicity of ω_e with respect to k_1 and k_2 can be obtained as

$\partial\omega_e/\partial k_1 > 0$, $\partial\omega_e/\partial k_2 > 0$. From above investigations on the monotonic properties of u^c with respect to $\omega(=\omega_e)$ and ω_e with respect to k_1 and k_2, the relationship between u^c and k_1, k_2 for fixed d_{ye} can be derived as follows:

$$\frac{\partial u^c(k_1,k_2)}{\partial k_1} < 0, \quad \frac{\partial u^c(k_1,k_2)}{\partial k_2} < 0 \quad (d_{ye} = const.) \qquad (6a,b)$$

Although d_{ye} defined by Eq. 4 can be regarded as a function of k_1 and k_1, d_{ye} can be understood as a constant value by choosing d_{y1} appropriately within the interval in Eq. 5c. From Eq. 6a, b, it can be observed that u^c increases when k_1 and k_2 decrease for any fixed value of d_{ye}. This monotonicity of u^c can be used to derive the upper bound of u^c with respect to the variation of uncertain parameters k_1, k_2, and d_{y1}. It should be noted that this monotonicity of u^c is not applicable to actual ground motions with randomness.

Consider the interval of the equivalent yield deformation d_{ye}. This is because u^c may be non-monotonic function of d_{ye} and it is useful to deal with d_{ye} directly in the uncertainty analysis. The upper and lower bounds of d_{ye} with respect to the interval parameters k_1, k_2, and d_{y1} can be derived from the interval arithmetic well known in the interval analysis as follows:

$$\underline{d}_{y1}\left(1+\underline{k}_1/\bar{k}_2\right) \le d_{ye} \le \bar{d}_{y1}\left(1+\bar{k}_1/\underline{k}_2\right) \qquad (7)$$

In Eq. 7, the variation of d_{ye} is limited by the upper and lower bounds. We suppose that three intervals of the interval of d_{ye}, called the intervals I–III, can be categorized as follows:

$$\begin{aligned}
&\underline{d}_{y1}\left(1+\underline{k}_1/\bar{k}_2\right) \le d_{ye} < \underline{d}_{y1}\left(1+\underline{k}_1/\underline{k}_2\right) && \text{[Interval I]}\\
&\underline{d}_{y1}\left(1+\underline{k}_1/\underline{k}_2\right) \le d_{ye} \le \bar{d}_{y1}\left(1+\underline{k}_1/\underline{k}_2\right) && \text{[Interval II]}\\
&\bar{d}_{y1}\left(1+\underline{k}_1/\underline{k}_2\right) < d_{ye} \le \bar{d}_{y1}\left(1+\bar{k}_1/\underline{k}_2\right) && \text{[Interval III]} \qquad (8)
\end{aligned}$$

where the lower bound of interval I coincides with that of the whole interval of d_{ye} in Eq. 7 and the upper bound of interval III coincides with that of interval of d_{ye}.

First, we consider the upper bound of u^c in interval II. Since the upper and lower bounds of d_{ye} are determined only by the difference of d_{y1} in the interval II, k_1 and k_2 can be given by the lower bounds as $k_1 = \underline{k}_1$, $k_2 = \underline{k}_2$ for any d_{ye} when d_{y1} is determined by the following equation:

$$d_{y1} = d_{ye}\frac{\underline{k}_2}{\underline{k}_1+\underline{k}_2} \qquad (9)$$

Since u^c is maximized at $k_1 = \underline{k}_1$, $k_2 = \underline{k}_2$ for fixed d_{ye} as explained in Eq. 6, it can be concluded that the upper bound of u^c in the interval II is derived by the combination of uncertain parameters in $k_1 = \underline{k}_1$, $k_2 = \underline{k}_2$, and d_{y1} in Eq. 9. **Figure 5** shows the conceptual diagram for determination of the upper

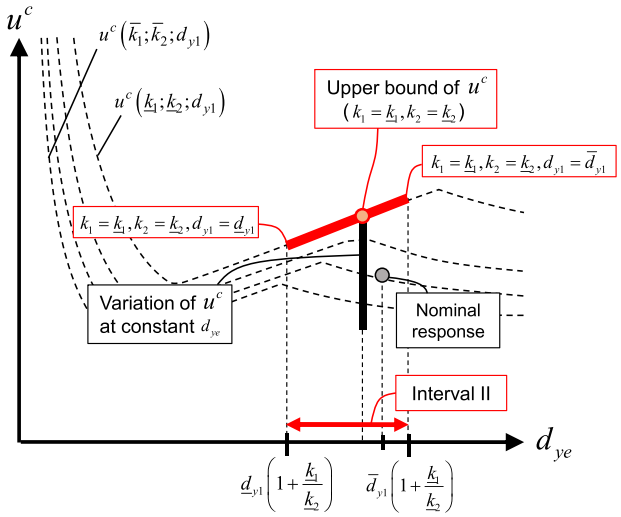

FIGURE 5 | Determination of upper bound of maximum elastoplastic displacement (interval II).

bound of u^c in the interval II. The categorized interval of d_{ye} in the intervals I–III is not related with the categorization of the interval due to the non-monotonicity property of u^c as shown in **Figure 2**. Therefore, the variation of the upper bound is varied according to the nominal design.

Secondly, the upper bounds of u^c in the interval I and III are investigated. In the interval I and III, k_1 and k_2 cannot be given by the lower bounds $k_1 = \underline{k}_1$, $k_2 = \underline{k}_2$. This is because the upper and lower bounds of d_{ye} in the interval I are determined so that d_{y1} reaches the lower bound of itself and those in the interval III are also calculated so that d_{y1} reaches the upper bound of itself. For example, when the upper bound of d_{ye} in the interval I is given by $k_1 = \underline{k}_1$, $k_2 = \underline{k}_2$, and $d_{y1} = \underline{d}_{y1}$, k_2 is needed to be increased to decrease d_{ye}. This can be easily understood from the definition of d_{ye} in Eq. 4. In this case, k_2 for a fixed value of d_{ye} can be described as follows:

$$k_2 = \frac{\underline{d}_{y1}}{d_{ye}-\underline{d}_{y1}}\underline{k}_1 \qquad (10)$$

In a similar way, the upper bound of u^c in the interval III can be derived by $k_2 = \underline{k}_2$, $d_{y1} = \bar{d}_{y1}$, and k_1 is given by the following equation:

$$k_1 = \frac{d_{ye}-\bar{d}_{y1}}{\bar{d}_{y1}}\underline{k}_2 \qquad (11)$$

Finally, the upper bound of $u^c(k_1;k_2;d_{y1})$, defined as $\bar{u}^c$, can be summarized as follows:

$$\bar{u}^c = \begin{cases} u^c\left(\underline{k}_1;\underline{d}_{y1}\underline{k}_1\Big/\left(d_{ye}-\underline{d}_{y1}\right);\underline{d}_{y1}\right) & \text{[Interval I]}\\ u^c\left(\underline{k}_1;\underline{k}_2;\underline{k}_2 d_{ye}\Big/\left(\underline{k}_2+\underline{k}_1\right)\right) & \text{[Interval II]},\\ u^c\left(\underline{k}_2\left(d_{ye}\Big/\bar{d}_{y1}-1\right)\underline{k}_2;\bar{d}_{y1}\right) & \text{[Interval III]} \end{cases} \qquad (12)$$

Figure 6 shows the diagram for determination of $\bar{u}^c$ with respect to the variation of k_1, k_2, and d_{y1}. The supremum value of the maximum critical elastoplastic displacement can be derived from the maximum value of $\bar{u}^c$.

Evaluation of Upper Bound of Maximum Elastoplastic Displacement at Base-Isolation Story

The supremum value of the upper bound of the maximum displacement derived in the previous section corresponds to the maximum displacement of the superstructure including the deformation of the base-isolation story. However, the maximum deformation at the base-isolation story may be needed in the practical design. To apply the proposed method to evaluate the response of the base-isolation story, the maximum displacement u_I^c at the base-isolation story is obtained in this section by using u^c derived for the equivalent SDOF model.

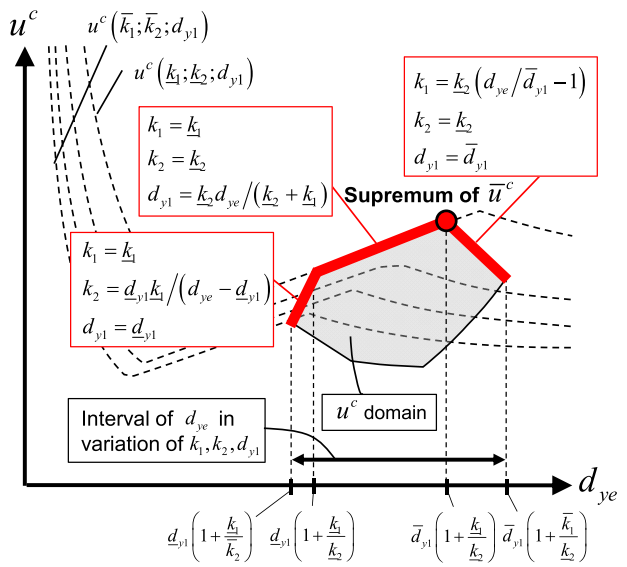

FIGURE 6 | Determination of upper bounds and supremum value of maximum elastoplastic displacement for critical double impulse.

Figure 7 shows the comparison of the restoring-force characteristics of the 2DOF model and the SDOF model. In the case where the base-isolation story yields after the first or second impulse, the plastic deformations of the 2DOF model and the equivalent SDOF model is the same. This is because the superstructure in the 2DOF model is assumed to be elastic. In this case, u_I^c can be estimated as shown in **Figure 7A**. In **Figure 7A**, $u^{(1)}$ and $u_I^{(1)}$ denote the maximum deformation of the equivalent SDOF model after the first impulse and that at the base-isolation story of the 2DOF model, respectively, and $u^{(2)}$ and $u_I^{(2)}$ represent those after the second impulse. Furthermore, $u_p^{(1)}$ and $u_{\mathrm{pI}}^{(1)}$ denote the maximum plastic deformation of the equivalent SDOF model after the first impulse and that at the base-isolation story of the 2DOF model, respectively, and $u_p^{(2)}$ and $u_{\mathrm{pI}}^{(2)}$ represent those after the second impulse. On the other hand, in the case where the base-isolation story is elastic even after the impulse input, u_I^c can be determined as shown in **Figure 7B**. Therefore, $u_I^c \equiv \max\{u_I^{(1)}, u_I^{(2)}\}$ can be evaluated by using Eq. 2 as follows:

$$u_I^c(\omega_e; d_{\mathrm{ye}}; d_{y1}) = \begin{cases} 2d_{y1}V/\omega_e d_{\mathrm{ye}} & (0 < V \le V_y/2) \\ \frac{2}{\omega_e^2 d_{\mathrm{ye}}}V^2 - \frac{1}{2}d_{\mathrm{ye}} + d_{y1} & (V_y/2 < V \le V_y) \\ \frac{1}{\omega_e}V + \frac{1}{2}d_{\mathrm{ye}} + d_{y1} & (V_y < V \le (\sqrt{3}+1)V_y) \\ \frac{1}{2\omega_e^2 d_{\mathrm{ye}}}V^2 - \frac{1}{2}d_{\mathrm{ye}} + d_{y1} & ((\sqrt{3}+1)V_y < V) \end{cases} \quad (13)$$

Consider the upper bound of u_I^c, defined as $\bar{u}_I^c$, with respect to the variation of k_1, k_2, and d_{y1}. As a similar formulation to derive $\bar{u}^c$ in Eq. 12, the monotonicity of u_I^c with respect to k_1 and k_2 cannot be introduced under the constraint that d_{ye} is constant. This is because it is needed to use d_{y1} and d_{ye} in the estimation of u_I^c from u^c and d_{y1} is a function of k_1 and k_2 to keep d_{ye} constant. Therefore, $\bar{u}_I^c$ is derived approximately by substituting the critical combination of k_1, k_2, and d_{y1} in Eq. 12 into the relation of u_I^c with u^c in Eq. 13.

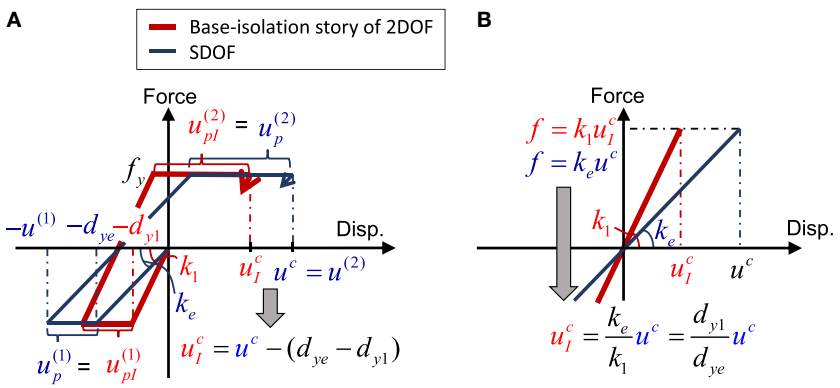

FIGURE 7 | Estimation of maximum elastoplastic deformation at base-isolation story through comparison of restoring force–displacement relations: (A) case: $u^{(1)} < u^{(2)}$: both plastic, (B) case: $u^{(1)}$, $u^{(2)}$: both elastic.

ROBUSTNESS EVALUATION USING ROBUSTNESS FUNCTION BASED ON INFO-GAP MODEL

In this section, the robustness function (Ben-Haim, 2006) is introduced to evaluate the robustness of a base-isolated high-rise building by using the supremum response of $\bar{u}^c$ and $\bar{u}_I^c$ derived in the previous section. The robustness in this paper is defined as the ability to keep the structural performance within a certain range under uncertainty of structural parameters. As shown in **Figure 8**, if the variation of performance is relatively small for the variation of design parameters **X**, the robustness of the structure is evaluated as high. However, in the case where the nominal responses are different in various nominal designs, it is difficult to compare the robustness of each nominal design.

To evaluate the robustness of a structure, Ben-Haim (2006) proposed the robustness function as a quantitative index. By applying the info-gap model to the uncertain parameters in the 2DOF model, the non-probabilistic interval parameters of k_1, k_2, and d_{y1} can be defined in the real coordinate space R as follows:

$$K_1(\alpha) = \left\{ k_1 \in R \,\middle|\, \tilde{k}_1 - \alpha\Delta k_1 \le k_1 \le \tilde{k}_1 + \alpha\Delta k_1, k_1 > 0 \right\}$$
$$K_2(\alpha) = \left\{ k_2 \in R \,\middle|\, \tilde{k}_2 - \alpha\Delta k_2 \le k_2 \le \tilde{k}_2 + \alpha\Delta k_2, k_2 > 0 \right\}$$
$$D_1(\alpha) = \left\{ d_{y1} \in R \,\middle|\, \tilde{d}_{y1} - \alpha\Delta d_{y1} \le d_{y1} \le \tilde{d}_{y1} + \alpha\Delta d_{y1}, d_{y1} > 0 \right\} \quad (14a,b,c)$$

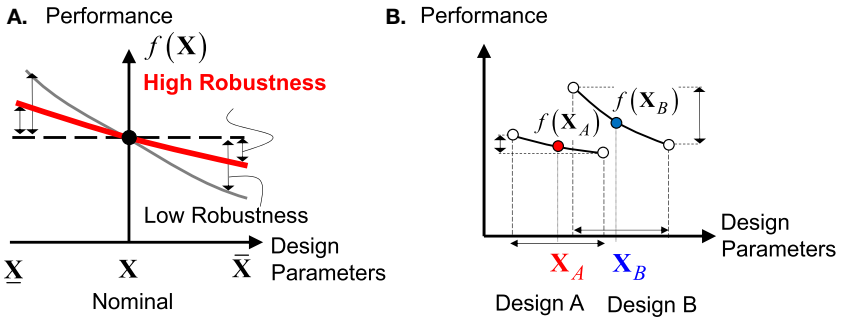

FIGURE 8 | Comparison of robustness for different nominal designs: (A) difference of robustness for the same nominal design, (B) difference of nominal design.

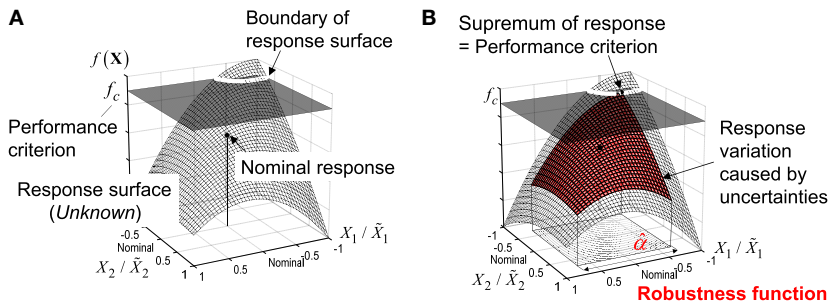

FIGURE 9 | Concept of robustness function: (A) nominal design and performance criterion, (B) determination of robustness function.

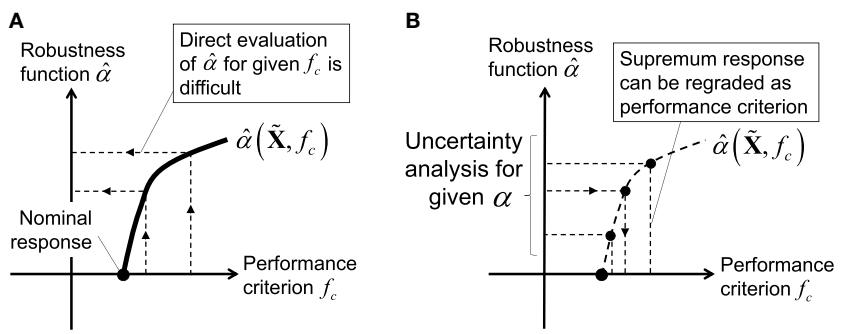

FIGURE 10 | Practical computation of robustness function: (A) original procedure of specifying performance criterion and (B) inverse procedure of specifying robustness function.

where $\alpha \geq 0$ denotes the variable range level, i.e., amplitude, of an interval parameter. The upper tilde symbol indicates the nominal value and the variations Δk_1, Δk_2, Δd_{y1} are normalized at $\alpha = 1$.

The robustness function $\hat{\alpha}$ is defined as the maximum value of α with which the performance requirement is satisfied for uncertain parameters $\mathbf{X}(\alpha)$ described as follows:

$$\hat{\alpha}(\tilde{\mathbf{X}}, f_c) = \max\{\alpha | \max\{f(k_1, k_2, d_{y1}) | k_1 \in K_1(\alpha), k_2 \in K_2(\alpha), d_{y1} \in D_1(\alpha)\} < f_c\} \quad (15)$$

where f and f_c denote a function of structural performance, e.g., the maximum interstory drift, and the performance criterion of f, respectively. **Figure 9** shows the concept of determining the robustness function. As shown in **Figure 9B**, when the supremum of the maximum response caused by the variation of the seismic response due to the uncertainty of $K_1(\alpha)$, $K_2(\alpha)$, and $D(\alpha)$ reaches the performance criterion f_c, the robustness function $\hat{\alpha}$ can be determined. In the case for $\hat{\alpha} = 0$, f_c can be regarded to correspond to the nominal response $f(\tilde{\mathbf{X}})$. The larger value of $\hat{\alpha}$ means that the current nominal structural design has a larger robustness to uncertainties for satisfying the constraint given by the specified value of f_c.

For the practical computation of the robustness function $\hat{\alpha}$, it is known that the direct computation of $\hat{\alpha}$ for given value of f_c is difficult due to the need of iterative calculation as shown in **Figure 10A**. On the other hand, by regarding the maximum value of f, i.e., the supremum of the objective function, for a given value of α as f_c in $\hat{\alpha} - f_c$ relation, the robustness function $\hat{\alpha}$ can be obtained as shown in **Figure 10B**. In this practical procedure of computing the robustness function, the supremum value of the structural response, e.g., the maximum elastoplastic displacement, can be evaluated as shown in the Section "Evaluation of Upper Bound of Maximum Elastoplastic Displacement at Base-Isolation Story."

NUMERICAL EXAMPLES

Numerical examples are presented for a 30-story base-isolated building model to evaluate the robustness concerned with the maximum elastoplastic displacement. To show the accuracy of the upper bound derived in Eq. 12, the upper and lower bounds of the maximum elastoplastic displacement derived in the proposed formulations are compared with the maximum elastoplastic displacements generated by the Monte Carlo simulation (MCS) where the stiffness and yield deformation at the base-isolation story and the stiffness of the superstructure are randomly generated as uncertain parameters. Then, the robustness functions in terms of the supremum value of the maximum elastoplastic displacements of the overall structure and that of the base-isolation story are evaluated for various yield deformations. In particular, the robustness evaluation for different nominal designs with different yield deformations at the base-isolation story is performed to derive a preferable robust design for the base-isolated high-rise building model.

Consider a 30-story base-isolated building and introduce a 2DOF model as shown in **Figure 3**. The mass of each story in the superstructure is 2.0×10^6 kg, i.e., $m_2 = 6.0 \times 10^7$ kg. The stiffness k_2 of the superstructure is given so that the fundamental natural period of the superstructure with fixed base is 3.0 s, i.e., $k_2 = 2.63 \times 10^8$ N/m. The mass of the base-isolation story is $m_1 = 6.0 \times 10^6$ kg. It is assumed that NRBs and U-shaped steel dampers are installed at the base-isolation story. The restoring-force characteristic of the combination of the natural rubber isolators and the U-shaped steel dampers is assumed to be elastic–perfectly plastic and this modeling enables the application of the critical response of an elastic–perfectly plastic model to the double impulse (Kojima and Takewaki, 2015). The yield deformation at the base-isolation story is treated as the target design parameter and given by $\tilde{d}_{y1} = 0.01$, 0.02, 0.03, and 0.04 m. The initial stiffness k_1 of the base-isolation story is given so that the fundamental natural period of the model with a rigid superstructure is 1.0 s, i.e., $k_1 = 2.61 \times 10^9$ N/m. The reference uncertainties of Δk_1, Δk_1, and Δd_{y1} are determined as $\Delta k_1 = 0.2\tilde{k}_1$, $\Delta k_2 = 0.05\tilde{k}_2$, and $\Delta d_{y1} = 0.2\tilde{d}_{y1}$.

Figure 11 shows examples of the variation of the upper and lower bounds of the critical elastoplastic deformation for $\tilde{d}_{y1} = 0.01$ and 0.02 m and $V = 1.0$ m/s with respect to the equivalent yield deformation. The dotted two lines represent the variation of the relation u^c–d_{ye} for $k_1 = 0.8\tilde{k}_1$, $k_2 = 0.95\tilde{k}_2$ (upper dotted line) and $k_1 = 1.2\tilde{k}_1$, $k_2 = 1.05\tilde{k}_2$ (lower dotted line), respectively. It can be observed from this figure that the variation of u^c is different

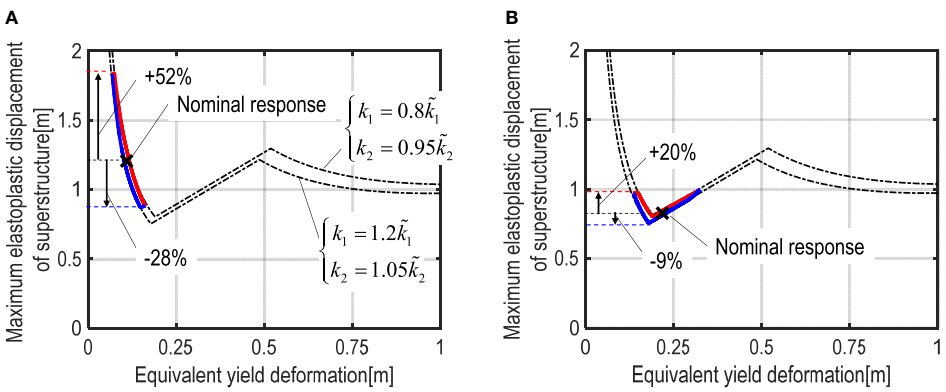

FIGURE 11 | Upper and lower bounds of critical elastoplastic displacement of superstructure: (A) $\tilde{d}_{y1} = 0.01$ and (B) $\tilde{d}_{y1} = 0.02$.

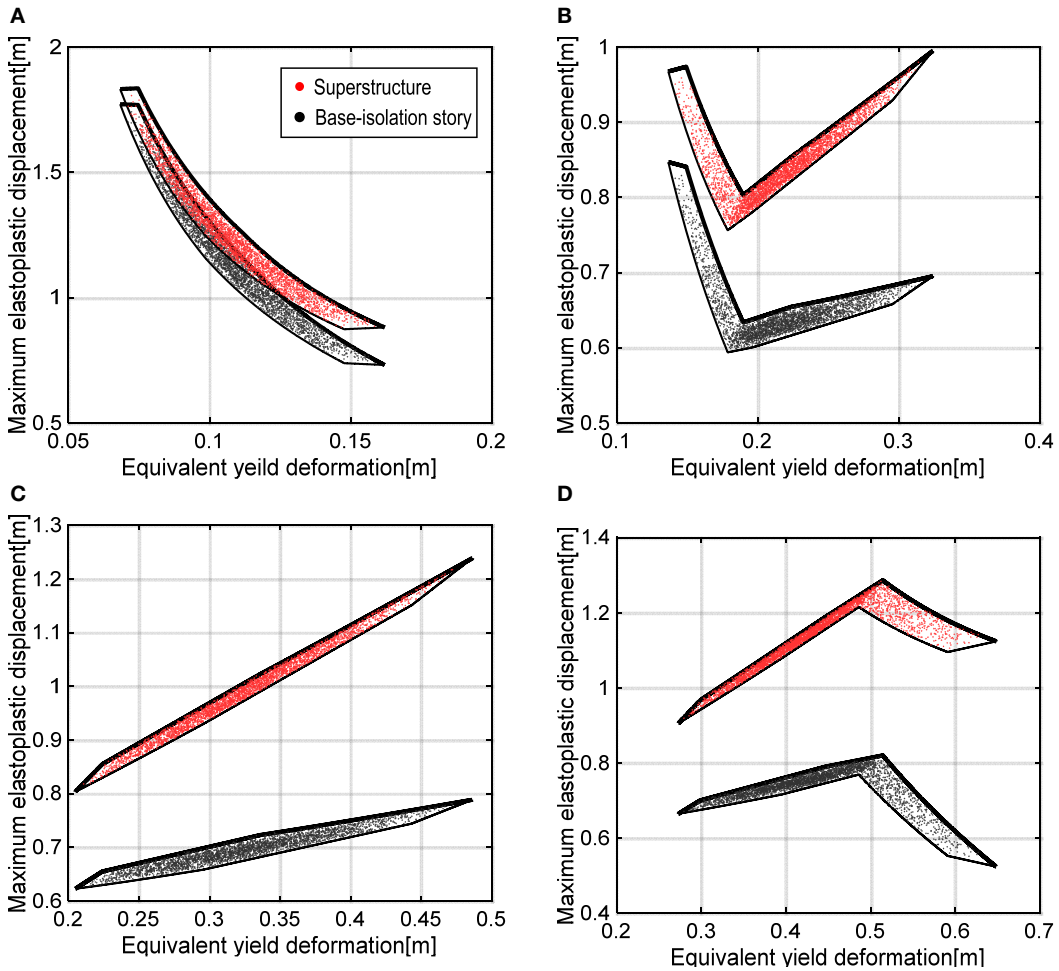

FIGURE 12 | Comparison of variations of maximum elastoplastic displacement: (A) $\tilde{d}_{y1} = 0.01$, (B) $\tilde{d}_{y1} = 0.02$, (C) $\tilde{d}_{y1} = 0.03$, and (D) $\tilde{d}_{y1} = 0.04$.

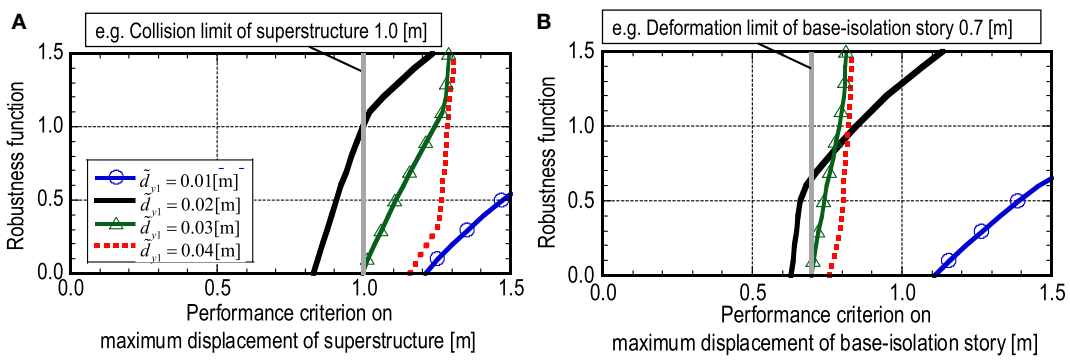

FIGURE 13 | Comparison of robustness functions for maximum displacement of models with various nominal yield deformations: (A) superstructure and (B) base-isolation story.

for different $\tilde{d}_{y1}$, i.e., the variation ratio to the nominal response for $\tilde{d}_{y1} = 0.01\ m$ is $\bar{u}^c/\tilde{u}^c = 1.52$, $\underline{u}^c/\tilde{u}^c = 0.72$, and that for $\tilde{d}_{y1} = 0.02$ m is $\bar{u}^c/\tilde{u}^c = 1.20$, $\underline{u}^c/\tilde{u}^c = 0.91$.

To examine the accuracy of the upper bounds of u^c and u_I^c derived in this paper, **Figure 12** shows the comparison of the variation of u^c and u_I^c for randomly selected uncertain models with the upper and lower bounds of u^c and u_I^c. The random models are generated by the MCS, where k_1, k_2, and d_{y1} are produced randomly by using the probabilistic density function based on the normal distribution. As shown in these figures, the maximum

elastoplastic displacements u^c and u_I^c of any models in the interval of d_{ye} are enveloped by $\bar{u}^c$ and $\bar{u}_I^c$.

Figure 13 shows the comparison of the robustness functions of $\bar{u}^c$ and $\bar{u}_I^c$ for different $\tilde{d}_{y1}$ and $V = 1.0$ m/s. To evaluate the robustness of the structure, we focused on the specified performance criterion. For example, if the limit maximum displacement of the superstructure is 1.0 m and the limit maximum elastoplastic deformation of the base-isolation story is 0.7 m, the robustness function for $\tilde{d}_{y1} = 0.02\,m$ is the largest in these models. This is because, as shown in **Figure 12**, the non-monotonic variation of u^c is included in the range of variation of d_{ye} for $\tilde{d}_{y1} = 0.02\,m$ where the maximum elastoplastic deformations of the overall structure after the first and second impulses coincide. From these observations, it can be concluded that there exists a preferable design of the yield deformation d_{y1} at the base-isolation story from the view point of the robust design.

CONCLUSION

A new method for evaluating the structural robustness of an elastoplastic base-isolated high-rise building has been proposed where the closed-form expression (Kojima and Takewaki, 2015) on the maximum elastoplastic deformation of an SDOF system under the critical double impulse is used. Since this closed-form expression on the critical response is based on the SDOF model, a 2DOF model with simultaneous uncertainties of the structural parameters has been transformed into an equivalent elastoplastic SDOF model. The elastic stiffness and yield deformation of the base-isolation story and the stiffness of the superstructure have been chosen as uncertain parameters.

In the closed-form formulation of the maximum elastoplastic deformation, there exists a non-monotonicity property of the critical elastoplastic deformation with respect to the yield deformation. The robustness function based on the info-gap model (Ben-Haim, 2006) has been introduced to measure the robustness quantitatively. The equivalent yield deformation in the SDOF model has been selected as a key uncertain parameter in the info-gap model. To find the worst scenario of the elastoplastic response, we have proposed the classified three different domains in this interval of the equivalent yield deformation. In each domain of the equivalent yield deformation, the upper bound of the maximum elastoplastic response has been derived by investigating the combination of the structural uncertain parameters where the two parameters can be fixed at the edges of interval, i.e., an upper or lower bound of the interval parameter, and another one parameter is varied according to the fixed equivalent yield deformation.

The robustness function has been evaluated by using the supremum value of the maximum elastoplastic displacement. In addition to the evaluation of the maximum displacement of the equivalent SDOF model, i.e., the displacement of the overall structure, the robustness of the displacement at the base-isolation story has been studied. Although the robustness evaluation considering the elastoplastic structural responses seems to be difficult due to the large amount of computational load by the time-history response analysis, this was overcome by using the closed-form expression explained above.

A 30-story base-isolated building model has been investigated as a numerical example where the yield deformation at the base-isolation story was treated as the principal design parameter. The robustness functions for the supremum value of the elastoplastic displacement at the overall structure and the base-isolation story have been evaluated in these building models with different yield deformations at the base-isolation story. It has been shown that a preferable nominal yield deformation design exists in the base-isolated high-rise building to make the robustness in terms of the elastoplastic structural response larger. This is because the variation of the structural response due to the simultaneous uncertainties may be small in the domain where the maximum displacement after the first impulse and that after the second impulse coincide at the specified equivalent yield deformation. It may be concluded that the proposed method is useful for finding preferable design parameters leading to higher robustness of elastoplastic base-isolated high-rise buildings.

AUTHOR CONTRIBUTIONS

KF carried out the theoretical and numerical analysis. KY carried out the numerical investigation. YK suggested theoretical formulation. IT supervised the theoretical analysis.

FUNDING

Part of the present work is supported by the Grant-in-Aid for Scientific Research (KAKENHI) of Japan Society for the Promotion of Science (No. 15H04079, 16K18184, and 26420545). This support is greatly appreciated.

REFERENCES

Ben-Haim, Y. (2006). *Information-Gap Decision Theory: Decisions under Severe Uncertainty*, 2nd Edn. London: Academic Press.

Ben-Haim, Y., Chen, G., and Soong, T. T. (1996). Maximum structural response using convex models. *J. Eng. Mech.* 122, 325–333. doi:10.1061/(ASCE)0733-9399(1996)122:4(325)

Ben-Haim, Y., and Elishakoff, I. (1990). *Convex Models of Uncertainty in Applied Mechanics*. Amsterdam: Elsevier.

Elishakoff, I., and Ohsaki, M. (2010). *Optimization and Anti-Optimization of Structures under Uncertainty*. London: Imperial College Press.

Fujita, K., and Takewaki, I. (2011). An efficient methodology for robustness evaluation by advanced interval analysis using updated second-order Taylor series expansion. *Eng. Struct.* 33, 3299–3310. doi:10.1016/j.engstruct.2011.08.029

Fujita, K., and Takewaki, I. (2012). Robustness evaluation on earthquake response of base-isolated buildings with uncertain structural properties under long-period ground motions. *Architectoni.ca J.* 1, 46–59. doi:10.5618/arch.2012.v1.n1.5

Guo, S. X., and Li, Y. (2013). Non-probabilistic reliability method and reliability-based optimal LQR design for vibration control of structures with uncertain-but-bounded parameters. *Acta Mech. Sinica* 29, 864–874. doi:10.1007/s10409-013-0068-4

Han, R., Li, Y., and Lindt, J. (2014). Seismic risk of base isolated non-ductile reinforced concrete buildings considering uncertainties and mainshock-aftershock sequences. *Struct. Saf.* 50, 39–56. doi:10.1016/j.strusafe.2014.03.010

Kanno, Y., and Takewaki, I. (2006). Robustness analysis of trusses with separable load and structural uncertainties. *Int. J. Solids Struct.* 43, 2646–2669. doi:10.1016/j.ijsolstr.2005.06.088

Kanno, Y., and Takewaki, I. (2016). Robustness analysis of elastoplastic structure subjected to double impulse. *J. Sound Vib.* 383, 309–323. doi:10.1016/j.jsv.2016.07.023

Kanno, Y., Yasuda, K., Fujita, K., and Takewaki, I. (2017). Robustness of SDOF elastoplastic structure subjected to double-impulse input under simultaneous uncertainties of yield deformation and stiffness. *Int. J. Non Linear Mech.* 91, 151–162. doi:10.1016/j.ijnonlinmec.2017.02.013

Kojima, K., and Takewaki, I. (2015). Critical earthquake response of elastic-plastic structures under near-fault ground motions (part 1: fling-step input). *Front. Built Env.* 1:12. doi:10.3389/fbuil.2015.00012

Matsuda, Y., and Kanno, Y. (2008). Robustness analysis of structures based on plastic limit analysis with uncertain loads. *J. Mech. Mate. Struct.* 3, 213–242. doi:10.2140/jomms.2008.3.213

Naeim, F., and Kelly, J. M. (1999). *Design of Seismic Isolated Structures*. New York: Wiley.

Qiu, Z., and Wang, X. (2003). Comparison of dynamic response of structures with uncertain but bounded parameters using non probabilistic interval analysis method and probabilistic approach. *Int. J. Solids Struct.* 40, 5423–5439. doi:10.1016/S0020-7683(03)00282-8

Roy, B. K., Chakraborty, S., and Mihsra, S. K. (2012). Robust optimum design of base isolation system in seismic vibration control of structures under uncertain bounded system parameters. *J. Vib. Cont.* 20, 786–800. doi:10.1177/1077546312466577

Takewaki, I. (2008). Robustness of base-isolated high-rise buildings under code-specified ground motions. *Struct. Design Tall Spec. Build.* 17, 257–271. doi:10.1002/tal.350

Takewaki, I., and Ben-Haim, Y. (2005). Info-gap robust design with load and model uncertainties. *J. Sound Vib.* 288, 551–570. doi:10.1016/j.jsv.2005.07.005

Taniguchi, R., Kojima, K., and Takewaki, I. (2016a). Critical response of 2DOF elastic-plastic building structures under double impulse as substitute of near-fault ground motion. *Front. Built Environ.* 2:2. doi:10.3389/fbuil.2016.00002

Taniguchi, R., Kojima, K., and Takewaki, I. (2016b). "Critical response of 2DOF elastic-plastic building structures under double impulse," in *The Summaries of Technical Papers of Annual Meeting of Architectural Institute of Japan, Structures I* (Tokyo: Architectural Institute of Japan (AIJ)), 407–408. (in Japanese).

Tsompanakis, Y., Lagaros, N. D., and Papadrakakis, M. (2008). *Structural Design Optimization Considering Uncertainties*. London: Taylor & Francis.

Yang, C., Tangaramvong, S., Gao, W., and Tin-Loi, F. (2015). Interval elastoplastic analysis of structures. *Comp. Struct.* 151, 1–10. doi:10.1016/j.compstruc.2014.12.004

Yang, C., Tangaramvong, S., Tin-Loi, F., and Gao, W. (2017). Influence of interval uncertainty on the behavior of geometrically nonlinear elastoplastic structures. *J. Struct. Eng.* 143. doi:10.1061/(ASCE)ST.1943-541X.0001618

Conflict of Interest Statement: The authors declare that the research was conducted in the absence of any commercial or financial relationships that could be construed as a potential conflict of interest.

APPENDIX

Relationship between 2DOF Model and SDOF Model

Consider a base-isolated building structure as shown in **Figure A1** (the same as the model in **Figure 3**). It is often the case that base-isolated building structures are modeled into a simplified model. A 2DOF model is a good simplified model. However further simplification into an SDOF model is desirable because a closed-form solution (Kojima and Takewaki, 2015) can be used for the SDOF model under the double impulse.

Consider two SDOF models, i.e., SDOF (a) model (the same as the model in **Figure 3**) and SDOF (b) model under the double impulse. SDOF (a) model is a model with series springs and ignored base-isolation story mass and SDOF (b) model is a model with rigid superstructure (**Figure A1**). For the SDOF (a) model, those equivalent quantities can be expressed as follows:

$$\begin{aligned} m_e &= m_2 \\ 1/k_e &= 1/k_1 + 1/k_2 \\ f_y &= k_1 d_{y1} = k_e d_{ye} \end{aligned} \tag{A1}$$

On the other hand, for the SDOF (b) model, those equivalent quantities can be expressed as follows:

$$\begin{aligned} m_e &= m_1 + m_2 \\ k_e &= k_1 \\ d_{ye} &= d_{y1} \end{aligned} \tag{A2}$$

Another possibility of modeling by modifying $m_e = m_2$ into $m_e = m_1 + m_2$ in the SDOF (a) model may be considered. However, this modification seems to influence the result slightly (smaller than 10% in high-rise base-isolated buildings as treated here). Furthermore, the series spring modeling in the SDOF (a) model appears compatible with the neglect of m_1.

For numerical simulations, consider a base-isolated N-story shear building model. The fundamental natural period of the superstructure with fixed base is given by $0.1 \times N$ (s). The stiffness k_2 is obtained from this condition. The floor mass per story is assumed to be 200×10^3 kg. Then $m_2 = 200 \times 10^3 \times N$ (kg).

The yield displacement of the base-isolation story is $d_{y1} = 0.03$ m. The fundamental natural period of the base-isolated building with rigid superstructure is given by 1.0 s (the stiffness is the sum of the isolators and steel dampers). The stiffness k_1 is obtained by this condition. The mass of the base-isolation story is $m_1 = 600 \times 10^3$ kg.

Figure A2 shows the comparison of the critical plastic deformation in the base-isolation story after the second impulse among the 2DOF model (time-history response analysis), the SDOF (a) model (series spring model and ignored base-isolation story mass) and the SODF (b) model (rigid superstructure model). The critical plastic deformation of the SDOF model after the second impulse was derived in the reference (Kojima and Takewaki, 2015). It can be observed that, while the SDOF (b) model with rigid superstructure is a better model for a low-rise building model ($N = 5$, 10), the SDOF (a) model with series springs and ignored base-isolation story mass is a better model for a high-rise building model ($N = 30$). It can also be observed that, for $N = 20$, the SDOF (a) model can simulate the response of the 2DOF model in the lower input level up to $V/V_y = 3$ and the response of SODF (b) model is more close to the actual response in the range of $V/V_y = 4$–5.

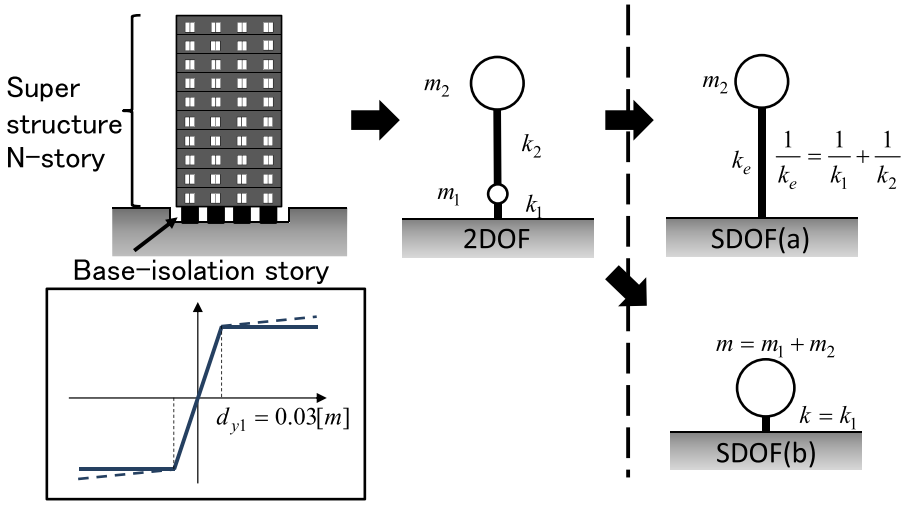

FIGURE A1 | Modeling of base-isolated building into single-degree-of-freedom (SDOF) model with series springs and ignored base-isolation story mass and SDOF model with rigid superstructure.

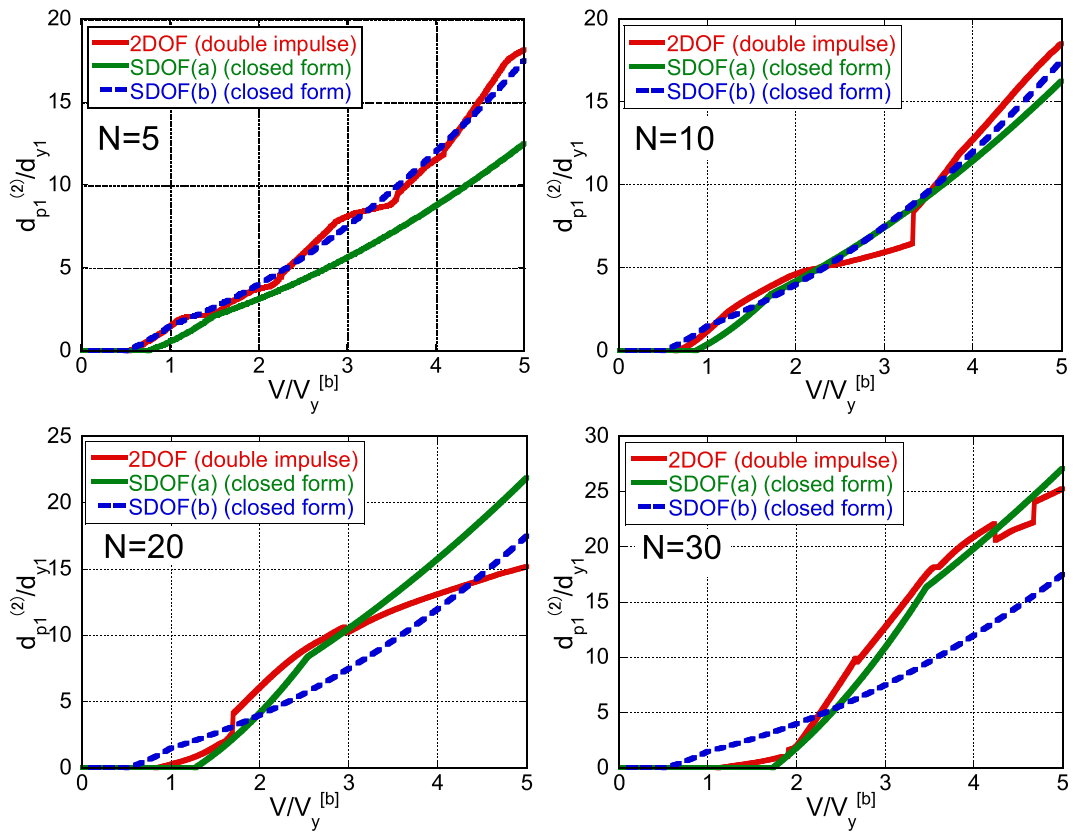

FIGURE A2 | Plastic deformation in base-isolation story in 5, 10, 20, and 30-story base-isolated buildings after the second impulse under double impulse with respect to input level (2DOF model, single-degree-of-freedom (SDOF) model (a) with series springs and SDOF model (b) with rigid superstructure).